PHYSICAL REVIEW B **84**, 100504(R) (2011)

Spatial inhomogeneity and planar symmetry breaking of the lattice incommensurate supermodulation in the high-temperature superconductor $Bi_2Sr_2CaCu_2O_{8+y}$

Nicola Poccia,[1] Gaetano Campi,[2] Michela Fratini,[1] Alessandro Ricci,[1] Naurang L. Saini,[1] and Antonio Bianconi[1,*]

[1]*Department of Physics, Sapienza University of Rome, P. le A. Moro 2, I-00185 Roma, Italy*

[2]*Institute of Crystallography, CNR, via Salaria Km 29.300, Monterotondo Stazione, I-00016 Roma, Italy*

(Received 2 August 2011; published 12 September 2011)

Using scanning micro-x-ray diffraction we report a mixed real and reciprocal space visualization of the spatial heterogeneity of the lattice incommensurate supermodulation in a single crystal of $Bi_2Sr_2CaCu_2O_{8+y}$ with $T_c = 84$ K. The mapping shows an amplitude distribution of the supermodulation with large lattice fluctuations at a microscale with ∼50% amplitude variation. The angular distribution of the supermodulation amplitude in the *a*-*b* plane shows a lattice chiral symmetry, forming a left-handed oriented striped pattern. The spatial correlation of the supermodulation is well described by a compressed exponential with an exponent of 1.5 ± 0.3 and a correlation length of ∼50 μm, showing intrinsic lattice disorder in high-temperature superconductors.

DOI: 10.1103/PhysRevB.84.100504 PACS number(s): 74.72.−h, 61.05.cf, 61.43.−j, 74.25.Jb

One of the emerging common features of high-temperature superconductors (HTSs) is the intrinsic lattice inhomogeneity,[1–4] but it remains practically unknown because of the lack of methods probing both the k space and the real space from the nanoscale to the microscale. The intrinsic lattice inhomogeneity is related to the coexistence of two or more electronic components showing a nanoscale phase separation in the normal phase.[3,4] In fact, two strongly correlated electronic components at the Fermi level are expected to exhibit a phase separation between two electronic phases with different charge densities.[5] The low-density phase is close to the Wigner localization limit in the normal phase and below T_c it forms a Bose-like condensate or a bipolaronic condensate in the presence of an electron-lattice interaction.[6,7] The high-density phase forms a BCS condensate below T_c, therefore the HTS phase appears to be at the BCS-Bose crossover in a multigap superconductor.[6,7] The striped superconductor showing a nanoscale phase separation of striped domains with different gaps has been called the "superstripes" i.e. a striped superconductor scenario, characterized at larger scales by a complex landscape of striped patches.[8]

In cuprates there is agreement on the experimental fact that the itinerant carriers induced by doping are injected in the oxygen $2p$ orbitals[9] and that at the Fermi level there are two main electronic components.[10]

(1) The nodal particles with a higher Fermi velocity with the wave vector on the Fermi surface arcs around the (π,π) direction of the reciprocal k space, i.e., moving nearly at 45° from the Cu-O bond direction: These states have molecular b_1 orbital symmetry composed of atomic oxygen $2p_{x,y}$ hybridized with a pure Cu $3d_{x^2-y^2}$ orbital.

(2) The antinodal particles with lower Fermi velocity with a Fermi wave vector in the $(0,\pi),(\pi,0)$ directions of the reciprocal k space: In the normal phase they show a pseudogap below T^*. These particles have strong coupling to the $B1g$ phonon.[11] This mode involves the Q_2 rhombic distortion of the CuO_4 platelet.[12] These particles run in the real space around the Cu-O bond direction and are made of a molecular orbital with a_1 symmetry composed of an oxygen $2p_{x,y}$ orbital hybridized with mixed Cu $3d_{3z^2-r^2}$ and $3d_{x^2-y^2}$ atomic orbitals. Their orbital symmetry has been determined by Cu $L_{2,3}$ polarized x-ray absorption near-edge spectroscopy (XANES) and the associated instantaneous pair distribution function of the Cu-O pairs by a polarized extended x-ray absorption fine structure (EXAFS), and they have been associated with pseudo Jahn-Teller polarons.[13]

The phase separation in cuprates with the formation of lattice domains with different charge densities has been clearly observed in the case of mobile dopants, oxygen interstitials in oxygenated La_2CuO_{4+y} both in the underdoped[14] and in the optimum doping[15,16] regime. In this case the domain growth and the density of the mobile oxygen interstitials are expected to track the hole density in the CuO_2 plane.

A second common feature of all HTSs is that their lattice architecture is a "heterostructure at an atomic limit" where atomic *layers* of a superconducting material are intercalated by block *layers*.[17] In these superlattices the lattice misfit between the different layers in cuprates,[18–22] pnictides,[23] and chalcogenides[24,25] plays a key role as the third variable in the phase diagram of the superconductors.

Most of the studies on electronic inhomogeneity have been focused on the system $Bi_2Sr_2CaCu_2O_{8+y}$ (Bi2212). In this system the misfit strain[18–22] between the block layers (Bi_2O_2-Sr_2O_2) and the bilayers (CuO_2-Ca-CuO_2) induces a lattice corrugation of both the BiO planes[26–29] and the CuO_2 planes,[30,31] appearing as a lattice supermodulation in x-ray diffraction that forms stripes of distorted and undistorted lattice Witan electronic structures reconstructed with multibands and broken Fermi surface arcs.[31–34] This lattice supermodulation has been recently associated with the modulation of the superconducting gaps,[35] revealing the effect of this specific lattice modulation on the superconducting CuO_2 layers.[30,31]

In this Rapid Communication we have investigated the spatial mapping of the variation of the amplitude of the superstructure lattice modulation with the specific wave vector $0.21b^*$, $0.5c^*$ in Bi2212 (Refs. 26–31) looking for a multiscale phase separation on the micrometer scale.[36,37] The nanoscale electronic and topological inhomogeneity in Bi2212 has been widely investigated by scanning tunneling microscopy and scanning tunneling spectroscopy (STM and STS).[35,38–41] The Fermi surface has been measured by techniques such as angle-resolved photoemission spectroscopy (ARPES).[10,42]

 ©2011 American Physical Society

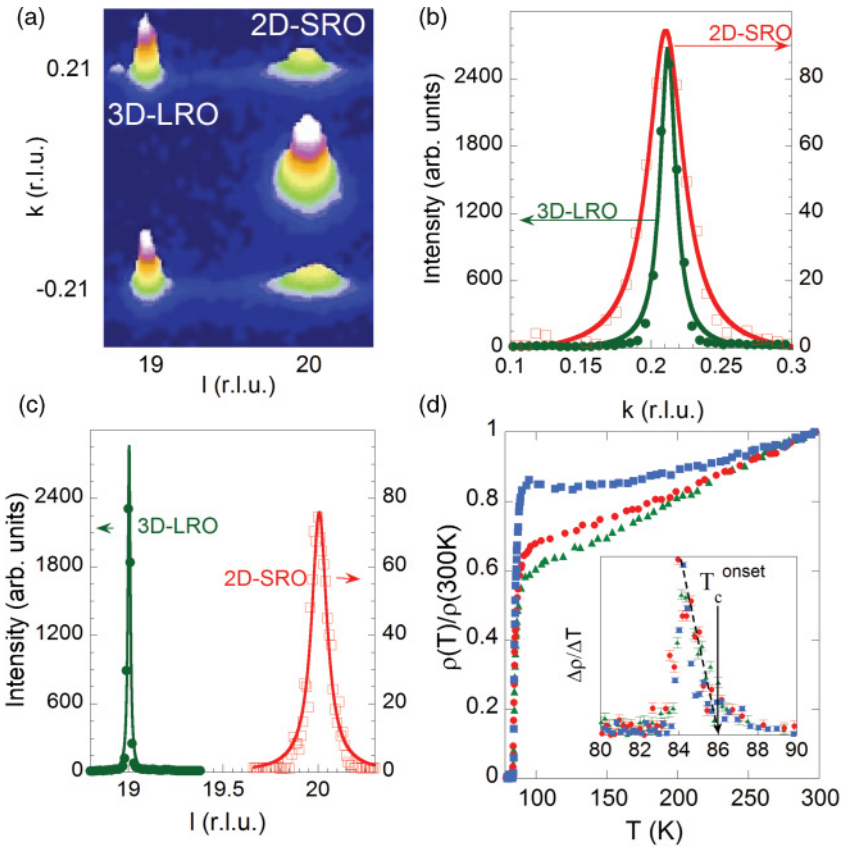

FIG. 1. (Color online) (a) X-ray diffraction pattern in the (k,l) plane of Bi2212 recorded by a CCD detector showing the 3D-LRO and 2D-SRO satellites near the (0,0,20) reflection. (b) and (c) show the profiles of the x-ray reflections due to the 2D-SRO (open rectangles) and 3D-LRO (filled circles) satellites along the c^* and b^* directions, where l and k are measured in the reciprocal lattice units (r.l.u), respectively. (d) Temperature-dependent resistivity of Bi2212 superconducting crystals used in this work (green triangles, red circles, and blue squares represent resistivity in the a, b, and c axes, respectively). The inset shows the resistivity derivatives around T_c. The black arrow shows the T_c onset of the superconducting transition.

The k-space information obtained from these methods is spatially averaged, and it is generally difficult to quantitatively reconcile these results with the nanoscale structure. Here, we have attempted to overcome this limit and used scanning micro-x-ray diffraction (μXRD). The results provide a mixed real and reciprocal space visualization of the spatial heterogeneity of the lattice incommensurate supermodulation in the Bi2212 system, showing quenched disorder and translational and rotational broken symmetry.

The μXRD experiment at the beamline (ID13) of the ESRF takes advantage of the focusing method of the 12-keV x-ray synchrotron radiation beam emitted by an 18-mm period undulator of the ESRF 6.03-GeV storage ring, operated in multibunch mode with a current of 200 mA. The beamline uses two monochromators positioned in series; the first is a liquid N_2 cooled Si-111 double crystal or Si-111 (bounce); the second is a channel cut monochromator employing a single liquid-nitrogen-cooled Si crystal. The optics of the microfocus beamline includes compound refractive lenses, Kirkpatrick Baez (KB) mirrors, and crossed Fresnel zone plates focusing the beam to a spot of 1 μm in diameter. The interaction volume with the crystal of the 1-μm beam is $1 \times 1 \times 20$ μm^3. The detector of x-ray diffraction images is a high resolution CCD camera (Mar CCD) with a point spread function 0.1 mm, 130-mm entrance window, and a 16-bit readout placed at a distance of ~90 mm from the sample. The measurements were made on a well-characterized Bi2212 single crystal of 100×130 μm^2 surface and 80 μm thickness, grown by the traveling-solvent-floating-zone method (TSFZ). The growth velocity was adopted to be 0.5 mm/h, and the growth atmosphere was a mixed gas flow of O_2 (20%) and Ar (80%). A structural analysis was performed using four-axis x-ray diffraction, and the basic structure of the samples was found to be orthorhombic symmetry with lattice parameters of $a \approx 542$ pm, $b \approx 547$ pm, $c = 3070$ pm, α and $\gamma \approx 90.0°$, $\beta \approx 92°$, with a large orthorhombic distortion in the range 0.5%–1.1%, in agreement with other overdoped crystals grown by the TSFZ technique.[43,44] The investigated samples are overdoped with an oxygen content y determined to be $\sim 0.26 \pm 0.01$, corresponding to a hole density of ~0.21 holes per Cu site.[45] The crystal was mounted on a XY mechanical translator for scanning parallel to the crystallographic (a,b) plane. The experimental setup in x-ray reflection mode allows the xy translation of the sample with 4.97-μm steps in the x and y directions.

A typical diffraction pattern of synchrotron x-ray reflections due to satellite peaks near the main crystal reflection (0,0,20) is shown in Fig. 1(a). There are two distinct sets of incommensurate superstructures. The first is a three-dimensional long-range order (3D-LRO) modulation, characterized by a very sharp and resolution-limited peak, and the second is a two-dimensional (2D) short-range order (SRO) modulation, characterized by a diffuse profile in the c-axis direction due to 2D domain walls separating the 3D domains of 3D-LRO. For each Bragg refection the diffraction vector H can be written as $H = ha^* + kb^* + 1c^* + mq_s [q_s = \beta b^* + (1/\gamma)c^*, \gamma = 1]$.

The q_s vector, called the superstructure vector, is the wave vector of the modulation, defined as the linear combination of the base vectors of the three-dimensional reciprocal lattice $q_s = \alpha a^* + \beta b^* + \gamma c^*$. Figures 1(b)

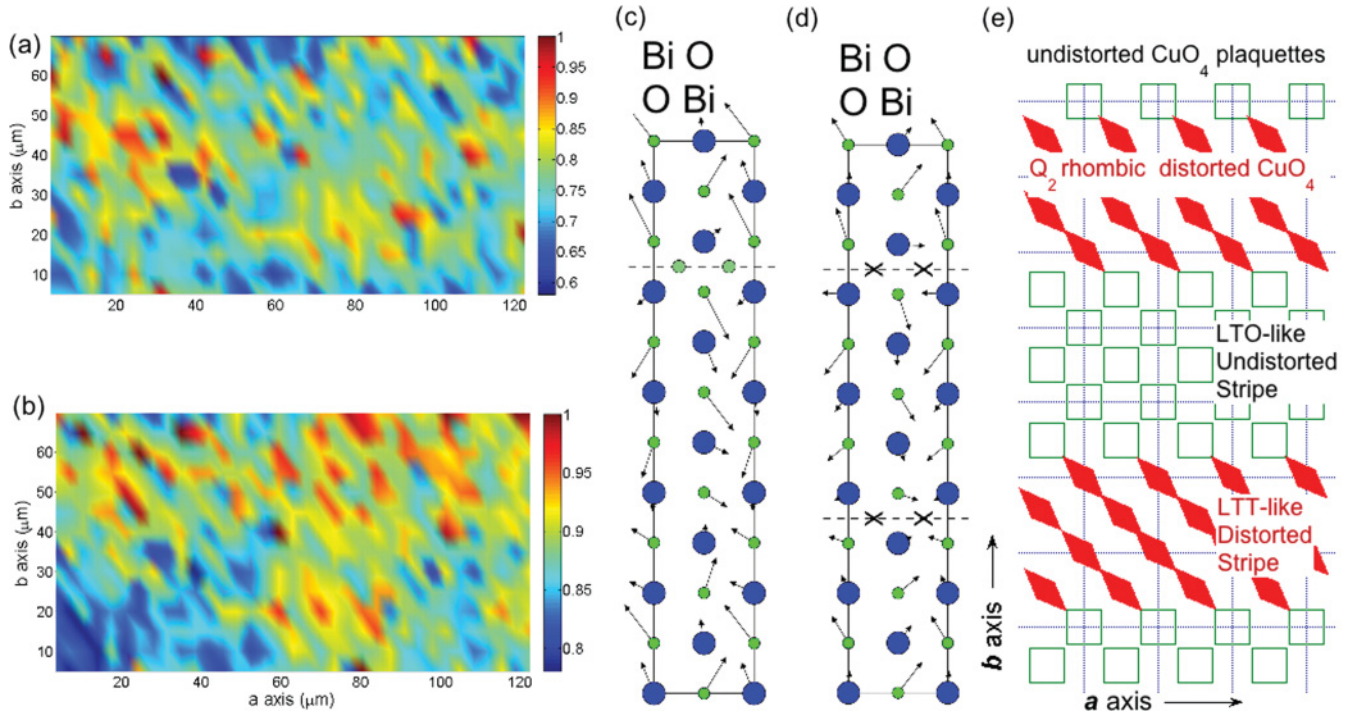

FIG. 2. (Color online) (a) and (b) The position-dependent intensities of the superstructure 3D-LRO (a) and the superstructure 2D-SRO (b) superstructure satellite reflections in Bi2212. The crystallographic ***a*** axis is along the horizontal direction, and the ***b*** axis is along the vertical direction. The very dark gray (blue color) indicates the weak supermodulation amplitude, and the light gray and dark gray (yellow and red) show the regions of high XRD superstructure reflections. (c) and (d) (from Refs. 46 and 47): Atomic displacements in the BiO layer projected into the *x*-*y* plane from the density functional theory (DFT) bulk calculation (Refs. 46 and 47) (c) and the experimental data by diffraction (see, e.g. Ref. 28); dashed lines are mirror planes, and ×'s mark points of stability found for the oxygen interstitials by DFT (d). (e) shows the topological distribution of lattice stripes in the CuO_2 plane of the BI2212 plane probed by Cu *K*-edge resonant x-ray diffraction (Ref. 30) and by Cu *K*-edge EXAFS (Ref. 31). The open squares (filled rhombs) indicate undistorted (distorted) CuO_4 plaquettes in the undistorted (distorted) stripes. The rhombs due to atomic Q_2 local lattice distortion of the square CuO_4 plaquette could order in the right-handed or the left-handed direction, breaking the rotational symmetry of the lattice. The figure shows the left-handed orientation of the Q_2 rhombic distortions with the direction of the Cu-O bond elongation of the distorted CuO_4 plaquette at 45° from the direction of the supermodulation parallel to the vertical direction.

and 1(c) show the profiles of the x-ray scattering reflections $(h,4-n\times\tau,l)$ for $\tau = 0.21$. The experimental diffraction coherence lengths are $\xi_c^{3D} = 1/\Delta L = 944 \pm 2$ nm; $\xi_b^{3D} = 1/\Delta k = 190 \pm 2$ nm and $\xi_c^{2D} = 1/\Delta L = 146 \pm 5$ nm; $\xi_b^{2D} = 1/\Delta K = 82 \pm 5$ nm, where Δl, Δk are the full width of half maximum (FWHM) of the diffraction reflection profiles, respectively, for the 3D-LRO and 2D-SRO, distinguishing the long-range order from the short-range order.

The *x*-*y* position dependence of the integrated satellite peak intensity [Figs. 2(a) and 2(b)] shows that the co-existing 2D-SRO and 3D-LRO structural modulations are quite inhomogeneous on the micrometer scale. The position dependence of the 3D-LRO and 2D-SRO satellites is shown in Figs. 2(a) and 2(b), respectively. The color scales from very dark gray (blue color) for the very weak supermodulation amplitude, and the light gray and dark gray (yellow and red) for large supermodulation amplitude. The intensity (satellite superstructure intensity integrated over square subareas of the CCD detector) is normalized with respect to the background intensity (I_o) of the tail of the main crystalline reflections. The ordered patches of 3D-LRO and 2D-SRO are oriented along one specific direction (left direction), 45° with respect to the vertical direction (the superlattice direction), implying two different diagonal directions (left and right) in the real space. This result provides clear evidence of the spontaneous breaking of the rotational crystal symmetry in the plane.

It was known that the atomic displacements in the BiO layers[26–29] run in the diagonal direction, as confirmed by *ab initio* calculations.[46,47] Cu *K*-edge resonant x-ray diffraction at the Cu *K* edge have shown that the CuO_2 plane is decorated by stripes of distorted and undistorted lattices in Bi2212 (Ref. 30) and the polarized EXAFS data[48,49] have shown that anomalous Cu-O-Cu bonds (45° from the superlattice direction) appear along only one of the two (left-handed or right-handed) diagonal directions as shown in Fig. 2(c). The broken rotational symmetry has also been observed later by STM experiments.[41]

The present evidence of left-handed microscale inhomogeneity of the lattice supermodulation intensity fluctuations provides evidence for broken lattice symmetry on a scale that is three orders of magnitude larger than seen previously. This result confirms the proposed intrinsic multiscale structural complexity driven from the nanoscale to the microscale by elastic fields[36,37] in a popular model cuprate system.

In Figs. 3 and 4 we quantify the observed inhomogeneity of the 3D-LRO and 2D-SRO superstructures by plotting the

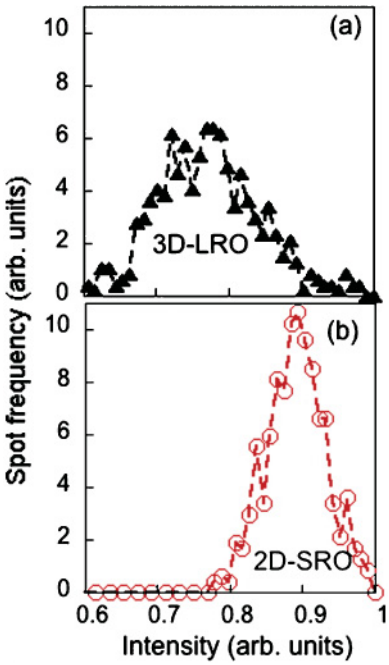

FIG. 3. (Color online) The intensity distribution of the 3D-LRO reflection intensities (filled triangles) (a) and 2D-SRO (open circles) (b) for the 120×70 μm^2 sample surface region.

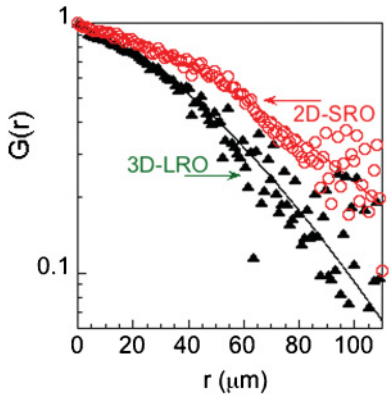

FIG. 4. (Color online) The spatial correlation function $G(r)$ of the x-ray diffraction intensities of the 3D-LRO superstructure reflections (filled triangles) and of the x-ray 2D-SRO reflections (open circles) recorded by micro-XRD mapping at the spots on the surface of the sample. The solid lines show the fitting with the curves $G(r) = \langle G(\vec{r})\rangle \propto A\exp[-r/\lambda]^{1.5}$ with correlation lengths $\lambda = 47$ and 78 μm for the 3D-LRO and the 2D-SRO, respectively.

distribution of intensities and the distance-dependent intensity correlations. Figure 3 shows that the mean values of the amplitude of the 3D-LRO and 2D-SRO are different, and the deviation from the average for both supermodulations is ~50%–60%. Also, over a small 50-μm area the amplitude of the micro-XRD reflection fluctuations are of the order of 30%. The large disorder of the amplitude of supermodulation can be assigned to the spatial inhomogeneity due to space variable stoichiometry that strongly deviates from the nominal composition.

The spatial correlation function $G(r)$ calculated following Ref. 15 is plotted in Fig. 3(c). The results show that the spatial correlation function can be described by a compressed exponential $G(r) = \langle G(\vec{r})\rangle \propto A\exp[-r/\lambda]^{\beta}$ with the same exponent $\beta = 1.5 \pm 0.3$ and with a cutoff in the range of 30–80 μm. These spatial correlation lengths between corrugated domains are much larger than the domain size measured by the planar diffraction coherence lengths $\xi_b^{2D} = 82$ nm and $\xi_b^{3D} = 190$ nm. The compressed exponential relaxation has been observed for a variety of soft matter systems undergoing "jamming" transitions such as collective dynamics with $\beta > 1$ (Ref. 50) instead of liquidlike fluctuations with $\beta < 1$. It should be recalled that an exponent of 1.5 has been reported for a nematic liquid crystal on a surface[51] and for granular matter.[52]

We have shown that the mixed k-space and real-space visualizations of the Bi2212 lattice shed light on the multiscale complexity in the HTS. These results contribute to the debate on rotational symmetry breaking observed by experimental methods by measuring the response of the average structure over micrometer-sized probed domains.[53–58] The large space variability in the amplitude of the lattice supermodulation underlines the high level of lattice disorder, implying a disorder in the electronic structure. In particular, small partial gaps due to the band folding determined by the striped lattice structure (superstripes)[8] could be masked by spatial fluctuations of the lattice corrugation that break the translational symmetry. In fact, a variation of 40% in the amplitude of the structural one-dimensional modulation should make a fuzzy landscape of partial gaps and complex multiple Fermi surfaces. The left-handed distribution of the superstructure fluctuation amplitude gives a chiral symmetry at the micrometer scale that is correlated with the breaking of the rotational symmetry of the rhombic Q_2 distortions of the CuO_4 platelets already observed by EXAFS and resonant diffraction.[6–11,38] The misfit strain between the superconductor and the spacer layers[18–21] is proposed to be the external field that breaks the symmetry between the right-handed and the left-handed orientation of the Q_2 distortions.[12,13] The present data support the multiscale breaking of rotational symmetry at the microscale as well as at the previously observed atomic scale. Moreover, these results introduce an alternate scenario of percolating microscopic superconducting domains in a preferential direction in a typical high-temperature superconductor. The scenario emerging from this experiment reminds the case of liquid-liquid phase separation,[59] like in smectic liquids or supercooled water, driven in cuprates by the pseudo Jahn Teller polarons (of Q2 type as shown in Fig. 23) that manifests itself at a micrometer scale with a broken rotational symmetry of the lattice texture.

The authors are grateful to Ginestra Bianconi for discussions and suggestions, and data analysis by using methods of statistical physics. We thank Manfred Burghammer and the ID13 beamline staff at ESRF for experimental help.

*antonio.bianconi@uniroma1.it

[1] E. Dagotto, Science **309**, 257 (2005)
[2] A. R. Bishop, J. Phys. Conf. Ser. **108**, 012027 (2008).
[3] K. A. Müller, J. Phys. Condens. Matter **19**, 251002 (2007).
[4] A. Bianconi, Physica C **235–240**, 269 (1994); A. Bianconi, D. Di Castro, G. Bianconi, A. Pifferi, N. L. Saini, F. C. Chou, D. C. Johnston, and M. Colapietro, *ibid*. **341–348**, 1719 (2000).
[5] K. I. Kugel, A. L. Rakhmanov, A. O. Sboychakov, N. Poccia, and A. Bianconi, Phys. Rev. B **78**, 165124 (2008).
[6] A. Bianconi, Solid State Commun. **91**, 1 (1994); A. Bianconi and M. Missori, *ibid*. **91**, 287 (1994).
[7] D. Innocenti, N. Poccia, A. Ricci, A. Valletta, S. Caprara, A. Perali, and A. Bianconi, Phys. Rev. B **82**, 184528 (2010).
[8] A. Bianconi, Int. J. Mod. Phys. B **14**, 3289 (2000); N. L. Saini and A. Bianconi, *ibid*. **14**, 3649 (2000).
[9] A. Bianconi, A. Congiu Castellano, M. De Santis, P. Rudolf, P. Lagarde, A. M. Flank, and A. Marcelli, Solid State Commun. **63**, 1009 (1987).
[10] A. Lanzara, P. V. Bogdanov, X. J. Zhou, S. A. Kellar, D. L. Feng, E. D. Lu, T. Yoshida, H. Eisaki, A. Fujimori, K. Kishio, J.-I. Shimoyama, T. Noda, S. Uchida, Z. Hussain, and Z.-X. Shen, Nature (London) **412**, 510 (2001).
[11] T. Cuk, F. Baumberger, D. H. Lu, N. Ingle, X. J. Zhou, H. Eisaki, N. Kaneko, Z. Hussain, T. P. Devereaux, N. Nagaosa, and Z.-X. Shen, Phys. Rev. Lett. **93**, 117003 (2004).
[12] Y. Seino, A. Kotani, and A. Bianconi, J. Phys. Soc. Jpn. **59**, 815 (1990).
[13] A. Bianconi, N. L. Saini, A. Lanzara, M. Missori, T. Rossetti, H. Oyanagi, H. Yamaguchi, K. Oka, and T. Ito, Phys. Rev. Lett. **76**, 3412 (1996).
[14] J. D. Jorgensen, B. Dabrowski, Shiyou Pei, D. G. Hinks, and L. Soderholm, B. Morosin, J. E. Schirber, E. L. Venturini, and D. S. Ginley, Phys. Rev. B **38**, 11337 (1988).
[15] M. Fratini, N. Poccia, A. Ricci, G. Campi, M. Burghammer, G. Aeppli, and A. Bianconi, Nature (London) **466**, 841 (2010).
[16] N. Poccia, M. Fratini, A. Ricci, G. Campi, L. Barba, A. Vittorini-Orgeas, G. Bianconi, G. Aeppli, and A. Bianconi, Nat. Mater. (London) (2011), doi: 1038/nmat3088.
[17] A. Bianconi Solid State Commun. **89**, 933 (1994).
[18] A. Bianconi, S. Agrestini, G. Bianconi, D. Castro, and N. Saini, in *Stripes and Related Phenomena*, edited by A. Bianconi and N. L. Saini, Selected Topics in Superconductivity Vol. 8 (Kluwer/Plenum New York, NY, 2000), Chap. 2, pp. 9–25.
[19] A. Bianconi, N. L. Saini, S. Agrestini, D. Di Castro, and G. Bianconi, Int. J. Mod. Phys. B **14**, 3342 (2000).
[20] A. Bianconi, D. Di Castro, N. L. Saini, and G. Bianconi, in *Phase Transitions and Self-Organization in Electronic and Molecular Networks*, edited by M. F. Thorpe and J. C. Phillips (Kluwer, Boston, MA, 2001), Chap. 24, p. 375.
[21] A. Bianconi, G. Bianconi, S. Caprara, D. D. Castro, H. Oyanagi, and N. L. Saini, J. Phys. Condens. Matter **12**, 10655 (2000).
[22] M Fratini, N. Poccia, and A. Bianconi, J. Phys. Conf. Ser. **108**, 012036 (2008).
[23] A. Ricci, N. Poccia, B. Joseph, L. Barba, G. Arrighetti, G. Ciasca, J. Q. Yan, R. W. McCallum, T. A. Lograsso, N. D. Zhigadlo, J. Karpinski, and A. Bianconi1, Phys. Rev. B **82**, 144507 (2010).
[24] A. Ricci, N. Poccia, B. Joseph, G. Arrighetti, L. Barba, J. Plaisier, G. Campi, Y. Mizuguchi, H. Takeya, Y. Takano, N. L. Saini, and A. Bianconi, Supercond. Sci. Technol. **24**, 082002 (2011).
[25] A. Ricci, N. Poccia, G. Campi, B. Joseph, G. Arrighetti, L. Barba, M. Reynolds, M. Burghammer, H. Takeya, Y. Mizuguchi, Y. Takano, M. Colapietro, N. L. Saini and A. Bianconi, Phys. Rev. B **84**, 060511 (2011).
[26] A. Yamamoto, M. Onoda, E. T. Muromachi, F. Izumi, T. Ishigaki, and H. Asano, Phys. Rev. B **42**, 4228 (1990).
[27] X. B. Kan and S. C. Moss, Acta Crystallogr. Sect. B **48**, 122 (1992).
[28] A. A. Levin, Y. I. Smolin, and Y. F. Shepelev, J. Phys. Condens. Matter **6**, 3539 (1994).
[29] D. Grebille, H. Leligny, and O. Pérez, Phys. Rev. B **64**, 106501 (2001).
[30] A. Bianconi, M. Lusignoli, N. L. Saini, P. Bordet, and P. G. Radaelli, Phys. Rev. B **54**, 4310 (1996).
[31] A. Bianconi, N. L. Saini, T. Rossetti, A. Lanzara, A. Perali, M. Missori, H. Oyanagi, H. Yamaguchi, Y. Nishihara, and D. H. Ha, Phys. Rev. B **54,** 12018 (1996).
[32] A. Perali, A. Bianconi, A. Lanzara, and N. L. Saini, Solid State Commun. **100**, 181 (1996).
[33] A. Bianconi, A. Valletta, A. Perali, and N. L. Saini, Solid State Commun. **102**, 369 (1997)
[34] A. Bianconi, A. Valletta, A. Perali, and N. L. Saini, Physica C **296**, 269 (1998).
[35] J. A. Slezak, J. Lee, M. Wang, K. McElroy, K. Fujita, B. M. Andersen, P. J. Hirschfeld, H. Eisaki, S. Uchida, and J. C. Davis, Proc. Natl. Acad. Sci. USA **105**, 3203 (2008).
[36] A. Saxena, Y. Wu, T. Lookman, S. Shenoy, and A. Bishop, Physica A (Amsterdam) **239**, 18 (1997).
[37] J. X. Zhu, K. H. Ahn, Z. Nussinov, T. Lookman, A. V. Balatsky, and A. R. Bishop, Phys. Rev. Lett. **91**, 057004 (2003).
[38] N. Jenkins, Y. Fasano, C. Berthod, I. Maggio-Aprile, A. Piriou, E. Giannini, B. W. Hoogenboom, C. Hess, T. Cren, and Ø. Fischer, Phys. Rev. Lett. **103**, 227001 (2009).
[39] A. Piriou, N. Jenkins, C. Berthod, I. Maggio-Aprile, and Ø. Fischer, Nat. Commun. **2**, 221 (2011).
[40] C. V. Parker, P. Aynajian, E. H. da Silva Neto, A. Pushp, S. Ono, J. Wen, Z. Xu, G. Gu, and A. Yazdani, Nature (London) **468**, 677 (2010).
[41] M. J. Lawler, K. Fujita, J. Lee, A. R. Schmidt, Y. Kohsaka, C. K. Kim, H. Eisaki, S. Uchida, J. C. Davis, J. P. Sethna, and Eun-Ah Kim, Nature (London) **466**, 347 (2010).
[42] N. L. Saini, J. Avila, A. Bianconi, A. Lanzara, M. C. Asensio, S. Tajima, G. D. Gu, and N. Koshizuka, Phys. Rev. Lett. **79**, 3467 (1997).
[43] I. Bdikin, A. N. Maljuk, A. B. Kulakov, C. T. Lin, P. Kumar, B. Kumar, G. C. Trigunayat, and G. A. Emel'chenko, Physica C **383**, 431 (2003).
[44] A. Maljuk, B. Liang, C. T. Lin, and G. A. Emelchenko, Physica C **355**, 140 (2001).
[45] T. Watanabe, T. Fujii, and A. Matsuda, Recent Res. Dev. Phys. **5**, 51 (2004).
[46] Y. He, S. Graser, P. J. Hirschfeld, and H. P. Cheng, Phys. Rev. B **77**, 220507 (2008).
[47] K. Foyevtsova, H. C. Kandpal, H. O. Jeschke, S. Graser, H. P. Cheng, R. Valentí, and P. J. Hirschfeld, Phys. Rev. B **82**, 054514 (2010).
[48] N. L. Saini, H. Oyanagi, M. Molle, K. Garg, C. Kim, and A. Bianconi, J. Phys. Chem. Solids **65**, 1439 (2004).
[49] N. L. Saini, A. Lanzara, A. Bianconi, and H. Oyanagi, Eur. Phys. J. B **18**, 257 (2000).

[50]O. G. Shpyrko, E. D. Isaacs, J. M. Logan, Y. Feng, G. Aeppli, R. Jaramillo, H. C. Kim, T. F. Rosenbaum, P. Zschack, M. Sprung, S. Narayanan, and A. R. Sandy, Nature (London) **447**, 68 (2007).

[51]M. Nespoulous, C. Blanc, and M. Nobili, Phys. Rev. Lett. **104**, 097801 (2010).

[52]P. Wang, C. Song, Y. Jin, K. Wang, and H. A. Makse, J. Stat. Mech: Theory Exp. **2010**, P12005.

[53]A. Kaminski, S. Rosenkranz, H. M. Fretwell, J. C. Campuzano, Z. Li, H. Raffy, W. G. Cullen, H. You, C. G. Olson, C. M. Varma *et al*., Nature (London) **416**, 610 (2002).

[54]S. V. Borisenko, A. A. Kordyuk, A. Koitzsch, T. K. Kim, K. A. Nenkov, M. Knupfer, J. Fink, C. Grazioli, S. Turchini, and H. Berger, Phys. Rev. Lett. **92**, 207001 (2004).

[55]M. Kubota, K. Ono, Y. Oohara, and H. Eisaki, J. Phys. Soc. Jpn. **75**, 053706 (2006).

[56]V. Arpiainen, A. Bansil and M. Lindroos, Phys. Rev. Lett. **103**, 067005 (2009).

[57]M. R. Norman, A. Kaminski, S. Rosenkranz, and J. C. Campuzano, Phys. Rev. Lett. **105**, 189701 (2010).

[58]R. Daou, J. Chang, D. LeBoeuf, O. Cyr-Choiniere, F. Laliberte, N. Doiron-Leyraud, B. J. Ramshaw, R. Liang, D. A. Bonn, W. N. Hardy, and Louis Taillefer, Nature (London) **463**, 519 (2010).

[59]D. Innocenti, A. Ricci, N. Poccia, G. Campi, M. Fratini, and A. Bianconi, J. Supercond. Nov. Magn. **22**, 529 (2009).